The Application of the Turkel–Zwas Explicit Large Time-Step Scheme to a Hemispheric Barotropic Model with Constraint Restoration*

I. M. NAVON**

Supercomputer Computations Research Institute, Florida State University, Tallahassee, FL 32306

R. DE VILLIERS

Mathematics and Dynamic Meteorology Division, NRIMS, CSIR, P.O. Box 395, Pretoria 0001, South Africa

(Manuscript received January 1985, in final form 4 December 1986)

ABSTRACT

The Turkel–Zwas (T–Z) explicit large time-step scheme addresses the issue of fast and slow time scales in shallow-water equations by treating terms associated with fast waves on a coarser grid but to a higher accuracy than those associated with the slow-propagating Rossby waves. The T–Z scheme has been applied for solving the shallow-water equations on a fine-mesh hemispheric domain, using realistic initial conditions and an increased time step. To prevent nonlinear instability due to nonconservation of integral invariants of the shallow-water equations in long-term integrations, we enforced a posteriori their conservation. Two methods, designed to enforce a posteriori the conservation of three discretized integral invariants of the shallow-water equations, i.e., the total mass, total energy and potential enstrophy, were tested. The first method was based on an augmented Lagrangian method (Navon and de Villiers), while the second was a constraint restoration method (CRM) due to Miele et al., satisfying the requirement that the constraints be restored with the least-squares change in the field variables. The second method proved to be simpler, more efficient and far more economical with regard to CPU time, as well as easier to implement for first-time users. The CRM method has been proven to be equivalent to the Bayliss–Isaacson conservative method. The T–Z scheme with constraint restoration was run on a hemispheric domain for twenty days with no sign of impending numerical instability and with excellent conservation of the three integral invariants. Time steps approximately three times larger than allowed by the explicit CFL condition were used. The impact of the larger time step on accuracy is also discussed.

1. Introduction

In recent years several approaches have been proposed for the efficient integration of the primitive equations numerical weather prediction models. In most of these methods the different time-scales of the advection and the gravity-inertia terms are dealt with separately in order to achieve computational efficiency. Examples are the semi-implicit schemes (see Robert, 1979; Burridge, 1975) and the split-explicit schemes (see Magazenkov et al., 1971; Gadd, 1978a, 1978b).

In the split-explicit schemes the horizontal advection terms in the governing equations are integrated with a time step limited by the wind speed, while the terms associated with gravity-inertia oscillations are integrated in a succession of shorter time steps; in this way a substantial computational economy is achieved when compared to usual explicit integration schemes.

A different and original approach was proposed by Turkel and Zwas (T–Z, 1979). Noting that the fast gravity–inertia waves contain only a small fraction of the total available energy and hence can be calculated with a lower accuracy than the slow Rossby waves, T–Z (1979) propose a space-splitting rather than a time-splitting for the shallow-water equations.

To be more explicit, they propose treating the terms associated with the fast gravity-inertia waves, on a coarser grid but to a higher accuracy than the terms associated with the slow Rossby waves. The relationship between the coarse and fine mesh is an integer $p > 1$, thus allowing, with little additional work, time-steps nearly p times larger than those allowed by the usual explicit stability criteria. While very promising as a concept, the T–Z scheme has not as yet been applied operationally with realistic initial conditions.

The purpose of this paper is to discuss the application of the T–Z space split-explicit integration schemes. For purposes of illustration, we consider the shallow-water equations on a hemispheric domain.

In section 2 we present the T–Z scheme for both a

* Contribution No. 244 of the Geophysical Fluid Dynamics Institute.

** Supported by the Florida State University Supercomputer Computations Research Institute which is partially funded by the U.S. Department of Energy through Contract No. DE-FC05-85ER250000.

limited-area Cartesian case and for the spherical case. In section 3 we present the new constraint restoration scheme for enforcing conservation of integral invariants. As the T–Z scheme applied to realistic initial conditions on the hemisphere did not conserve exactly the integral invariants of the shallow-water equations (a variation of 5%–10% in the potential enstrophy constraint), the restoration method due to A. Miele et al. (1969a,b, 1971) emerged as a simple and economical method, satisfying the requirement that the constraints be restored with the least-squares change of the variables. In section 4 the numerical results of long-term integrations on the hemisphere using the T–Z scheme are discussed, and the impact of the constraint restoration enforcing of integral invariants conservation is assessed. Computational efficiency and accuracy issues are also addressed. Conclusions are presented in section 5. Proofs of the stability condition for the T–Z scheme and the relationship between the CRM and the Bayliss–Isaacson method are presented in appendix A and appendix B, respectively.

2. The Turkel–Zwas explicit large time scheme for the shallow-water equations

a. *The Cartesian case*

The shallow-water equations in Cartesian coordinates can be written as

$$\begin{aligned} u_t + uu_x + vu_y + gh_x &= fv \\ v_t + uv_x + vv_y + gh_y &= -fu \\ h_t + uh_x + vh_y + h(u_x + v_y) &= 0, \end{aligned} \tag{1}$$

where u is the zonal wind, v the meridional wind, h the height, g the gravity and f the Coriolis parameter assumed constant for the subsequent analysis.

For a leap-frog explicit time integration with $\Delta x = \Delta y$ the stability condition is

$$\frac{\Delta t}{\Delta x} \leqslant \frac{1}{|u| + |v| + \sqrt{2gh}}, \tag{2}$$

and for typical meteorological conditions

$$\sqrt{gh} \gg (|u| + |v|), \tag{3}$$

while most of the energy is carried at the convective speed $O(|u| + |v|)$.

Turkel and Zwas (1979) identified the terms connected with the $\sqrt{gh}$ in the stability condition. They are the pressure gradient terms h_x and h_y in the momentum equations and the divergence term $h(u_x + v_y)$ in the continuity equation. Noting, however, the importance of the geostrophic departure in driving the whole system (see also Haltiner and Williams, 1980, pp. 51–52), Turkel and Zwas (1979) decided to treat the terms $(gh_x + fv)$ and $(gh_y + fu)$ as one entity and to calculate them on a coarse grid, but to compensate for the higher truncation error on the coarse grid by using a Padé compact difference approximation with fourth-order accuracy for their calculation.

We can express the Padé derivative operator as

$$\frac{\partial}{\partial x} \approx \frac{1}{\Delta x} \frac{\mu\delta}{1 + \delta^2/6}, \tag{4}$$

where the averaging and differencing operators, μ and δ respectively, are

$$\begin{aligned} \mu w_i &= \frac{1}{2}(w_{i+1/2} + w_{i-1/2}) \\ \delta w_i &= w_{i+1/2} - w_{i-1/2}. \end{aligned} \tag{5}$$

Application of the Padé differencing operator to the expression $gh_y + fu$ gives

$$g \frac{1}{\Delta y} \frac{\mu\delta}{(1 + \delta^2/6)} h_i + fu, \tag{6}$$

and upon clearing fractions we obtain

$$\begin{aligned} &\frac{g}{\Delta y}\mu\delta h_i + f(1 + \delta^2/6)u \\ &= \frac{1}{2}\left[\frac{g}{\Delta y}(h_{i+1} - h_{i-1}) + 2f\left(\frac{1}{6}u_{i+1} + \frac{2}{3}u_i + \frac{1}{6}u_{i-1}\right)\right]. \end{aligned} \tag{7}$$

Using all the information, the T–Z scheme (space-splitting scheme) takes the form of the following generalized leap-frog method:

$$\begin{aligned} u_{ij}^{n+1} = u_{ij}^{n-1} &- \lambda\Big[u_{ij}^n(u_{i+1,j}^n - u_{i-1,j}^n) + v_{ij}^n(u_{i,j+1}^n - u_{i,j-1}^n) \\ &+ \frac{g}{p}(h_{i+p,j}^n - h_{i-p,j}^n)\Big] \\ &+ 2\Delta t f\left[(1-\alpha)v_{ij}^n + \frac{\alpha}{2}(v_{i+p,j}^n + v_{i-p,j}^n)\right] \\ v_{ij}^{n+1} = v_{ij}^{n-1} &- \lambda\Big[u_{ij}^n(v_{i+1,j}^n - v_{i-1,j}^n) + v_{ij}^n(v_{i,j+1}^n - v_{i,j-1}^n) \\ &+ \frac{g}{p}(h_{i,j+p}^n - h_{i,j-p}^n)\Big] \\ &- 2\Delta t f\left[(1-\alpha)u_{ij}^n + \frac{\alpha}{2}(u_{i,j+p}^n + u_{i,j-p}^n)\right] \\ h^{n+1} = h^{n-1} &- \lambda\Big[u_{ij}^n(h_{i+1,j}^n - h_{i-1,j}^n) + v_{ij}^n(h_{i,j+1}^n - h_{i,j-1}^n) \\ &+ \frac{h_{ij}^n}{p}(u_{i+p,j}^n - u_{i-p,j}^n + v_{i,j+p}^n - v_{i,j-p}^n)\Big]. \end{aligned} \tag{8}$$

Here $\lambda = \Delta t/\Delta x = \Delta t/\Delta y$ and $p > 1$ is an integer which defines the relationship between the coarse mesh on which terms associated with the inertia–gravity waves are treated and the fine mesh on which terms associated with the slow Rossby waves are discretized.

With the original leap-frog method in the Cartesian case the incompressibility condition $u_x + v_y = 0$ is sat-

isfied exactly for the geostrophic Rossby wave. The difference scheme (8) no longer has this property and instead the divergence is zero only to the second order.

It is possible to insure that the divergence of the numerical solution is identically zero by appropriate averaging of the approximation to u_x in the y direction and v_y in the x direction. Turkel and Zwas (1979) found that averaging in the Cartesian case caused negligible changes in the accuracy.

The situation is different in the spherical case and will be elaborated on in the next section.

It can be proven that the stability criterion for this scheme where a leap-frog explicit time differencing method is employed is:

$$\frac{\Delta t}{\Delta x} \leqslant \frac{1}{|u|+|v|+\sqrt{2gh/p}}. \tag{9}$$

For proof of Eq. (9) see appendix A. Hence, one can use time-steps nearly p times larger than allowed by the usual explicit scheme.

If we use $\alpha = \frac{1}{3}$ in (8), we obtain the Padé difference approximation of (7), a fact which also emerges if we linearize (1) so as to obtain a linear system with constant coefficients and assume a solution of the form

$$\begin{pmatrix} u \\ v \\ h \end{pmatrix} = \begin{pmatrix} U \\ V \\ H \end{pmatrix} e^{i(\xi x+\eta y-\omega t)}. \tag{10}$$

Then, as shown by Turkel and Zwas (1979), the amplitudes corresponding to the numerical slow Rossby wave are

$$U = \frac{ig\eta H}{f}\left\{1+\frac{1}{2}\left(\alpha-\frac{1}{3}\right)(p\eta\Delta y)^2+\mathrm{O}[(p\eta\Delta y)^4]\right\}$$
$$V = \frac{ig\xi H}{f}\left\{1+\frac{1}{2}\left(\alpha-\frac{1}{3}\right)(p\xi\Delta x)^2+\mathrm{O}[(p\xi\Delta x)^4]\right\}. \tag{11}$$

Again choosing $\alpha = \frac{1}{3}$ gives us the fourth-order accuracy on the coarse mesh. This higher order on the coarse mesh grid will balance the second-order error of the convective terms on the fine mesh. This is the same α as predicted by the Padé approximation approach previously suggested.

Practical difficulties arise for a limited-area model at the boundaries when p, the ratio between the coarse and fine grids, is larger than 1. In such a case one has to formulate well-posed boundary conditions on an interpolated grid. We tested the feasibility of the method on a limited-area problem with doubly periodic boundary conditions, using $p = 5$ as done by Turkel and Zwas (1979) and obtained similar results to those reported by Turkel and Zwas.

b. *The spherical case*

The shallow-water equations on a sphere are given by

$$\frac{\partial u}{\partial t}+\frac{1}{a\cos\theta}\left[u\frac{\partial u}{\partial\lambda}+v\cos\theta\frac{\partial u}{\partial\theta}\right]-\left(f+\frac{u}{a}\tan\theta\right)v+\frac{g}{a\cos\theta}\frac{\partial h}{\partial\lambda}=0$$
$$\frac{\partial v}{\partial t}+\frac{1}{a\cos\theta}\left[u\frac{\partial v}{\partial\lambda}+v\cos\theta\frac{\partial v}{\partial\theta}\right]+\left(f+\frac{u}{a}\tan\theta\right)u+\frac{g}{a}\frac{\partial h}{\partial\theta}=0$$
$$\frac{\partial h}{\partial t}+\frac{1}{a\cos\theta}\left[\frac{\partial}{\partial\lambda}(hu)+\frac{\partial}{\partial\theta}(hv\cos\theta)\right]=0. \tag{12}$$

Here the Coriolis parameter f is nonconstant and is given by

$$f = 2\Omega\sin\theta, \tag{13}$$

where Ω is the rate of angular rotation of the earth, h is the height of the homogeneous atmosphere, u and v are the zonal and meridional wind components, while the latitudinal and longitudinal directions are given by θ and λ respectively, and a is the radius of the earth.

By using an analysis similar to that of Arakawa and Lamb (1977) for the linearized shallow-water equations system and considering solutions of the form:

$$(u,h)_{ij} = \mathrm{Re}\{u_j, h_j \exp[\hat{\imath}(ki\Delta\lambda-\sigma t)]\}, \tag{14}$$

where $\hat{\imath} = \sqrt{-1}$, k is the zonal wavenumber, σ is the gravity wave frequency,

$$\sigma = \pm\frac{(gH)^{1/2}\omega}{a\cos\theta\Delta\lambda}$$
$$\omega = \sin(k\Delta\lambda) \tag{15}$$

the maximum allowable time step for leap-frog explicit-time differencing and an A-type grid is (in the absence of Fourier high-latitude filtering)

$$\Delta t_{\max} = \frac{a\cos\theta\Delta\lambda}{(gH)^{1/2}\omega_{\max}} \tag{16}$$

(see also Takacs and Balgovind (1983)). The stability condition (16) depends on the space and time discretizations assumed, where H is the equivalent depth.

In our case $\omega_{\max} = 1$ for waves with wavelengths close to $4\Delta\lambda$. As in the Cartesian case, certain terms will be differenced over a coarser grid over points p meshes away in the λ (longitudinal) direction and q meshes away in the latitudinal direction θ. However, as can be seen from (16), the time restriction is dictated by the distance between mesh points in the longitudinal λ direction, namely the distance $a\cos\theta\Delta\lambda$. This is why Turkel and Zwas (1979) suggest taking p larger than q. They also suggest maintaining the averaging associated with the divergence term in the continuity equation.

The Turkel–Zwas scheme for the spherical case takes the following form:

$$u_{ij}^{n+1} = u_{ij}^{n-1} - \sigma\left[\frac{u_{ij}^n}{\cos\theta_j}(u_{i+1,j}^n - u_{i-1,j}^n) + v_{ij}^n(u_{i,j+1}^n - u_{i,j-1}^n) + \frac{g}{p\cos\theta_j}(h_{i+p,j}^n - h_{i-p,j}^n)\right]$$
$$+ 2\Delta t\left[(1-\alpha)\left(2\Omega\sin\theta + \frac{u_{ij}^n}{a}\tan\theta_j\right)v_{ij}^n + \frac{\alpha}{2}\left(2\Omega\sin\theta + \frac{u_{i+p,j}^n}{a}\tan\theta_j\right)v_{i+p,j}^n + \frac{\alpha}{2}\left(2\Omega\sin\theta_j + \frac{u_{i-p,j}}{a}\tan\theta_j\right)v_{i-p,j}^n\right]$$

$$v^{n+1} = v^{n-1} - \sigma\left[\frac{u_{ij}^n}{\cos\theta_j}(v_{i+1,j}^n - v_{i-1,j}^n) + v_{ij}^n(v_{i,j+1}^n - v_{i,j-1}^n) + \frac{g}{q}(h_{i,j+q}^n - h_{i,j-q}^n)\right]$$
$$- 2\Delta t\left\{(1-\alpha)\left(2\Omega\sin\theta_j + \frac{u_{ij}^n}{a}\tan\theta_j\right)u_{ij}^n\right.$$
$$\left. + \frac{\alpha}{2}\left[\left(2\Omega\sin\theta_{j+q} + \frac{u_{i,j+q}^n}{a}\tan\theta_{j+q}\right)u_{i,j+q}^n + \left(2\Omega\sin\theta_{j-q} + \frac{u_{i,j-q}^n}{a}\tan\theta_{j-q}\right)u_{i,j-q}^n\right]\right\}$$

$$h_{ij}^{n+1} = h_{ij}^{n-1} - \sigma\left\{\frac{u_{ij}^n}{\cos\theta_j}(h_{i+1,j}^n - h_{i-1,j}^n) + v_{ij}^n(h_{i,j+1}^n - h_{i,j-1}^n)\right.$$
$$+ \frac{h_{ij}^n}{\cos\theta_j}\left[(1-\alpha)(u_{i+p,j}^n - u_{i-p,j}^n) + \frac{\alpha}{2}(u_{i+p,j+q}^n - u_{i-1,j+q}^n + u_{i+p,j-q}^n - u_{i-p,j-q}^n)\right]\frac{1}{p}$$
$$+ \left[(1-\alpha)(v_{i,j+q}^n\cos\theta_{j+q} - v_{i,j-q}^n\cos\theta_{j-q}) + \frac{\alpha}{2}(v_{i+p,j+q}^n\cos\theta_{j+q}\right.$$
$$\left.\left. - v_{i+p,j-q}^n\cos\theta_{j-q} + v_{i-p,j+q}^n\cos\theta_{j+q} - v_{i-p,j-q}^n\cos\theta_{j-q})\right]\frac{1}{q}\right\} \quad (17)$$

where

$$\sigma = \Delta t/(a\cdot\Delta\lambda) = \Delta t/(a\cdot\Delta\theta). \quad (18)$$

For $\alpha = \frac{1}{3}$ the geostrophic balance and the incompressibility condition are satisfied to a higher order as was shown in the Cartesian case [Eq. (11)].

c. Treatment of polar regions for the Turkel–Zwas scheme

In what follows, we will assume that we are dealing with the Northern Hemisphere. Following Kalnay et al. (1983) we first transform the equations (12) using a stereographic projection, and then we area-average the equations over a polar cap. The stereographic projection of u and v results in unique u_p and v_p independent of the longitude λ (see also Takacs, 1986).

$$u_p = -u\sin\lambda - v\cos\lambda$$
$$v_p = u\cos\lambda - v\cos\lambda \quad (19)$$

Multiplying the u and v momentum equations in (12) by $\sin\lambda$ or $\cos\lambda$ and adding the products, results in:

$$\frac{\partial u_p}{\partial t} + \frac{1}{a\cos\theta}\left[u\frac{\partial u_p}{\partial\lambda} + v\cos\theta\frac{\partial u_p}{\partial\theta}\right] - fv_p$$
$$- \frac{g}{a\cos\theta}\left[\sin\lambda\frac{\partial h}{\partial\lambda} + \cos\lambda\frac{\partial h}{\partial\theta}\right] \quad (20a)$$

$$\frac{\partial v_p}{\partial t} + \frac{1}{a\cos\theta}\left[u\frac{\partial v_p}{\partial\lambda} + v\cos\theta\frac{\partial v_p}{\partial\theta}\right] + fu_p$$
$$- \frac{g}{a\cos\theta}\left[\cos\lambda\frac{\partial h}{\partial\lambda} + \sin\lambda\frac{\partial h}{\partial\theta}\right] \quad (20b)$$

$$\frac{\partial}{\partial t}h_p + \frac{1}{a\cos\theta}\left[\frac{\partial}{\partial\lambda}(hu) + \frac{\partial}{\partial\theta}(hv\cos\theta)\right] = 0. \quad (20c)$$

Let us consider integrating the transformed equations (20a)–(20c). The area of the polar cap A_c is

$$A_c = \int_0^{2\pi}\int_{\pi/2-\Delta\theta}^{\pi/2} a^2\cos\theta d\lambda d\theta = 2\pi a^2(1-\cos\Delta\theta). \quad (21)$$

If we start by integrating the continuity equation and area averaging

$$\frac{\partial\bar{h}p^{\Delta\theta}}{\partial t} = \frac{1}{A_c}\int_0^{2\pi}\int_{\pi/2-\Delta\theta}^{\pi/2}\left[\frac{\partial(hu)}{\partial\lambda} + \frac{\partial}{\partial\theta}(hv\cos\theta)\right]ad\theta d\lambda. \quad (22)$$

The first term vanishes since it is being integrated around a complete latitude circle (See Takacs, 1986). The second term becomes

$$\int_0^{2\pi}\int_{\pi/2-\Delta\theta}^{\pi/2}\frac{\partial}{\partial\theta}(hv\cos\theta)ad\lambda d\theta$$
$$= a\int_0^{2\pi}(hv\cos\theta)/d\lambda_{\pi/2-\Delta\theta} \quad (23)$$

which is approximated centered in finite-difference form as

$$a\int_0^{2\pi}(hv\cos\theta)/d\lambda = 2\pi\frac{a\sin\Delta\theta}{IM}\sum_{i=1}^{IM}(hv)_{i,j_{\text{pole}\pm1}}, \quad (24)$$

where IM is defined as the number of grid points in the zonal direction

$$\Delta\lambda = \frac{2\pi}{IM}. \tag{25}$$

By substituting into (22) we have

$$\frac{\partial \overline{hp}^{\Delta\theta}}{\partial t} = \frac{2\pi a \sin\Delta\theta}{2\pi a^2(1-\cos\Delta\theta)IM} \sum_{i=1}^{IM} (hv)_{i,j_{\text{pole}\pm 1}}$$

$$= \frac{\sin\Delta\theta}{aIM(1-\cos\Delta\theta)} \sum_{i=1}^{IM} (hv)_{i,j_{\text{pole}\pm 1}}. \tag{26}$$

For expressions with $q \neq 1$ in the Turkel–Zwas scheme, we repeat the process over a polar cap of $q\Delta\theta$ which gives a term

$$\frac{\partial \overline{h}_p^{\Delta\theta}}{\partial t} = \frac{\sin q\Delta\theta}{aIM(1-\cos q\Delta\theta)} \sum_{i=1}^{IM} (hv)_{i,j_{\text{pole}\pm q}}. \tag{27}$$

The same process is also applied to the transformed momentum equations in a manner similar to Takacs (1986).

d. Fourier filtering

Near the poles the longitudinal distances between neighboring points $\Delta x = a\cos\theta\Delta\lambda$ decreases as the poles are approached for a fixed $\Delta\lambda$.

Owing to these short distances and to fast moving inertia-gravity waves near the poles, prohibitively short time-steps are required to ensure computational stability. Different Fourier filtering or high-latitude filtering methods have been prosed for latitude–longitude global gridpoint models to allow the use of large time-steps. For a comprehensive survey see Takacs and Balgovind (1983).

In our experiments we have used the Arakawa and Lamb (1977) method in which the zonal pressure gradient and zonal mass flux terms are filtered. For the Turkel–Zwas scheme differencing gravity-wave related terms on a coarse grid over points p meshes away in the longitudinal direction results in a typical stability condition of the form

$$\frac{(gH)^{1/2}}{a\cos\theta} \sin\frac{(pk\Delta\lambda)}{p\Delta\lambda} \Delta t \leq 1 \tag{28}$$

or

$$\Delta t \leq \frac{(a\cos\theta)}{(gH)^{1/2}} \frac{p\Delta\lambda}{\sin(pk\Delta\lambda)} \tag{29}$$

or

$$\Delta t_{\max} = \frac{(a\cos\theta)p\Delta\lambda}{(gH)^{1/2}\omega_{\max}}, \tag{30}$$

where in our simplified case, $\omega_{\max} = 1$.

The increase in the maximum allowable time-step due to the differencing of gravity-wave related terms on a coarse grid has the following implications for high-latitude filtering. On one hand, on the coarser grid, the frequency of the fastest resolved propagating gravity mode, w_g decreases, but on the other hand we use a higher time-step.

As has been shown by Daley (1980), Takacs et al. (1985), the condition for the scheme to be linearly stable is

$$|w_g| \leq \frac{1}{\Delta t}. \tag{31}$$

The set of all gravity modes whose eigenfrequencies satisfy

$$|w_g| > \frac{1}{\Delta t} \tag{32}$$

constitutes the set of "fast" modes which will have to be Fourier filtered to maintain stability near the poles.

The coarse mesh differencing reduces the size of the fast modes set, but the use of a larger time step again increases the number of modes in the "fast" set [Eq. (32)], as defined by Daley (1980), meaning that as far as high-latitude filtering is concerned the same amount of effort will be required to maintain computational stability.

3. The constraint restoration method

a. Theory

The idea of enforcing a posteriori integral invariant conservation has been pursued by Sasaki (1976, 1977), as well as by Bayliss and Isaacson (1975) and Isaacson (1977). These ideas have been tested by Navon (1981). A new approach based on an augmented Lagrangian combined penalty-multiplier method has been proposed by Navon and de Villiers (1983).

In all these papers the solution to the finite-difference scheme is modified after a given number of time-steps (or at each time-step) so that certain functionals, representing the discrete integral invariants conservation relations, take prescribed values. Usually, the modification of the smallest norm to the value predicted by the finite-difference scheme at the given time-step is chosen.

It was pointed out by A. Miele (private communication) that an approach simpler than any of those mentioned above is available. This approach, called the constraint restoration algorithm, starts by assuming that the vector $\mathbf{x}$

$$\mathbf{x} = (\tilde{u}_{11}{}^n \cdots \tilde{u}^n_{N_xN_y}, \tilde{v}_{11}{}^n \cdots \tilde{v}^n_{N_xN_y}, \tilde{h}_{11}{}^n \cdots \tilde{h}^n_{N_xN_y}) \tag{33}$$

at the time $t = n\Delta t$, is in the vicinity of the optimal point $\mathbf{x}^*$, which satisfies the equality constraints

$$\phi(\mathbf{x}^*) = 0 \tag{34}$$

where

$$\phi(\mathbf{x}) = \begin{bmatrix} \phi_1(\mathbf{x}) \\ \vdots \\ \phi_r(\mathbf{x}) \end{bmatrix}, \quad r < 3N_xN_y = N. \tag{35}$$

Let us call $\mathbf{x}$ the *nominal point* not consistent with constraint (24), and let $\tilde{\mathbf{x}}$ denote a varied point (see also Miele and Heideman, 1968, Miele et al., 1969) related to the nominal point as follows:

$$\tilde{\mathbf{x}} = \tilde{\mathbf{x}} + \delta\mathbf{x}, \tag{36}$$

$\delta\mathbf{x}$ being a perturbation of $\mathbf{x}$ about the nominal point. By using quasilinearization, we obtain that equation (34) is approximated by

$$\phi(\mathbf{x}) + \delta\phi(\mathbf{x}) = 0, \tag{37}$$

where

$$\delta\phi(\mathbf{x}) = \mathbf{A}^{\mathrm{T}}(\mathbf{x})\delta\mathbf{x} \tag{38}$$

and where $\mathbf{A}(\mathbf{x})$ is the $N \times p$ matrix

$$\mathbf{A}(\mathbf{x}) = \begin{bmatrix} \frac{\partial\phi_1}{\partial x_1} & \frac{\partial\phi_2}{\partial x_1} & \cdots & \frac{\partial\phi_p}{\partial x_1} \\ \frac{\partial\phi_1}{\partial x_2} & \vdots & & \frac{\partial\phi_p}{\partial x_2} \\ \vdots & \vdots & & \\ \frac{\partial\phi_1}{\partial x_N} & \frac{\partial\phi_2}{\partial x_N} & & \frac{\partial\phi_p}{\partial x_N} \end{bmatrix}, \tag{39}$$

where the jth column is the gradient of ϕ_j with respect to the vector $\mathbf{x}$. We obtain the relation

$$\phi(\mathbf{x}) + \mathbf{A}^{\mathrm{T}}(\mathbf{x})\delta\mathbf{x} = 0 \tag{40}$$

from Eqs. (37) and (38).

In order to prevent the perturbation $\delta\mathbf{x}$ from becoming too large, we embed equation (40) into the one-parameter family of equations

$$\alpha\phi(\mathbf{x}) + \mathbf{A}^{\mathrm{T}}(\mathbf{x})\delta\mathbf{x} = 0, \tag{41}$$

α being a prescribed scaling factor in the range

$$0 \leqslant \alpha \leqslant 1. \tag{42}$$

If the position vector $\mathbf{x}$ is an approximation to the desired solution, we wish to restore constraint (34) while causing the least change in the coordinates of $\mathbf{x}$. Therefore we look for the minimum of the functional

$$J = \frac{1}{2}\delta\mathbf{x}^{\mathrm{T}}\delta\mathbf{x}, \tag{43}$$

subject to the linearized constraint (41).

As shown in Miele and Heideman (1968), by using standard methods of the theory of maxima and minima, the functional to be minimized is

$$F = \frac{1}{2}\delta\mathbf{x}^{\mathrm{T}}\delta\mathbf{x} + \lambda^{\mathrm{T}}[\phi(\mathbf{x}) + \mathbf{A}^{\mathrm{T}}(\mathbf{x})\delta\mathbf{x}], \tag{44}$$

where λ is the p component Lagrange multiplier vector:

$$\lambda = \begin{bmatrix} \lambda_1 \\ \vdots \\ \lambda_p \end{bmatrix}. \tag{45}$$

The optimum change $\delta\mathbf{x}$ is obtained when the gradient of the scalar function F with respect to the vector $\delta\mathbf{x}$ vanishes, i.e.

$$\delta\mathbf{x} = -\mathbf{A}(\mathbf{x})\lambda. \tag{46}$$

By combining equations (46) and (40) and eliminating $\delta\mathbf{x}$, we obtain an explicit expression for the Lagrange multiplier of the form:

$$\alpha\phi(\mathbf{x}) - \mathbf{B}(\mathbf{x})\lambda = 0, \tag{47}$$

where $\mathbf{B}(\mathbf{x})$ is the $p \times p$ matrix

$$\mathbf{B}(\mathbf{x}) = \mathbf{A}^{\mathrm{T}}(\mathbf{x})\mathbf{A}(\mathbf{x}). \tag{48}$$

In the case where $\mathbf{x}$ is a large vector (i.e. $N = 3N_xN_y \approx 10^4$) and p is a small number of constraints (in our case $p = 3$), we can easily calculate the Lagrange multipliers, i.e.

$$\lambda = \alpha\mathbf{B}^{-1}(\mathbf{x})\phi(\mathbf{x}). \tag{49}$$

From Eqs. (46) and (49) we obtain that the optimum restoration correction is given by

$$\delta\mathbf{x} = \alpha\mathbf{A}(\mathbf{x})\mathbf{B}^{-1}(\mathbf{x})\phi(\mathbf{x}). \tag{50}$$

If we define a scalar performance index

$$P = \phi^{\mathrm{T}}(\mathbf{x})\phi(\mathbf{x}), \tag{51}$$

then clearly, if $P = 0$, the vector $\mathbf{x}$ satisfies the equality constraints $\phi(\mathbf{x}) = 0$ and $P > 0$ otherwise.

By taking the first variation

$$\delta P = 2\phi^{\mathrm{T}}(\mathbf{x})\mathbf{A}^{\mathrm{T}}(\mathbf{x})\delta\mathbf{x} \tag{52}$$

of the performance index, and using relationship (41) Eq. (52) reduces to

$$\delta P = -2\alpha\phi^{\mathrm{T}}(\mathbf{x})\phi(\mathbf{x}) = -2\alpha P. \tag{53}$$

Since $P > 0$, Eq. (53) shows that for $\alpha > 0$ the first variation of the performance index is negative, and hence for small enough α the decrease of the performance index is guaranteed. The CRM method and the Bayliss–Isaacson (1975) conservative method are equivalent. For a proof of their equivalence see appendix B, and for a presentation of the Bayliss–Isaacson method see Navon (1981).

b. Scaling of the constraints

Due to the different physical units the integral constraints have different magnitudes. We therefore scaled the variables and the constraints so that after scaling they should be of similar magnitude and of order unity in the region of interest. We employed here the same method presented as in Navon and de Villiers (1983).

Here, $\mathbf{x}$ is a vector given by Eq. (33), while $\phi(\mathbf{x})$ is a three-component equality constraints vector

$$\phi(\mathbf{x}) = \begin{bmatrix} \phi_1 \\ \phi_2 \\ \phi_3 \end{bmatrix} = \begin{bmatrix} H^n - H^0 \\ Z^n - Z^0 \\ E^n - E^0 \end{bmatrix}, \tag{54}$$

where

$$\phi_1 = H^n - H^0 = \sum_{ij} h_{ij}^n \Delta x \Delta y - H^0$$

$$\phi_2 = Z^n - Z^0 = \frac{\Delta x \Delta y}{2} \times \sum_{ij} \frac{1}{h_{ij}} \left(\frac{v_{i+1,j}^n - v_{i-1,j}^n}{2\Delta x} - \frac{u_{i,j+1}^n - u_{i,j-1}^n}{2\Delta y} + f_j \right)^2 - Z^0$$

$$\phi_3 = E^n - E^0 = \frac{\Delta x \Delta y}{2} \sum_{ij} (u_{ij}^{n2} + v_{ij}^{n2} + g h_{ij}^n) h_{ij}^n. \quad (55)$$

Here H^n, Z^n and E^n are the values of the discrete integral invariants of mass, potential enstrophy and total energy at time $t_n = n\Delta t$, while H^0, Z^0 and E^0 are the values of the same integral invariants at the initial time $t = 0$.

The scaling can also be represented as a modified performance index by redefining

$$P = \phi^t W \phi \quad (56)$$

where W is a positive definite diagonal weight matrix given in our case by

$$\begin{pmatrix} L^{-1} & 0 & 0 \\ 0 & LV^{-2} & 0 \\ 0 & 0 & V^2 L^{-3} \end{pmatrix} \quad (57)$$

where L is the typical horizontal length, V typical velocity and we used a scaled time T as well

$$T = LV^{-1} \quad (58)$$

chosen so as to satisfy scaling constraints.

c. The constraint restoration algorithm

1) Assume a nominal point $\mathbf{x}$.

2) At the nominal point compute the constraint vector ϕ, the matrix $\mathbf{A}$ with equation (39) and matrix $\mathbf{B} = \mathbf{A}^T(\mathbf{x})\mathbf{A}(\mathbf{x})$ with equation (48), as well as the performance index P with equation (51).

3) Assume the restoration of step-size $\alpha = 1$ and determine $\delta\mathbf{x}$, using Eq. (50).

4) Compute the varied point $\tilde{\mathbf{x}}$ by

$$\tilde{\mathbf{x}} = \mathbf{x} + \delta\mathbf{x} \quad \text{[Eq. (36)]}. \quad (59)$$

5) At the varied point compute the performance index $\tilde{P}$. If $\tilde{P} < P$, the first iteration is completed and the scaling factor $\alpha = 1$ is acceptable. If this inequality is violated, i.e., $\tilde{P} > P$, instead of conducting a step-size search, Miele et al. (1969, 1971) propose a bisection process, i.e. α is bisected several times until the condition

$$\tilde{P} < P \quad (60)$$

is met. This is guaranteed by the descent property. [This means α must be replaced by some smaller value in the range (42)].

6) After a value of α in the range $0 \leqslant \alpha \leqslant 1$ has been found such that $\tilde{P} < P$, the first iteration is completed. The point $\tilde{\mathbf{x}} = \mathbf{x} + \delta\mathbf{x}$ is employed as the nominal point $\mathbf{x}$ for the second iteration; this procedure is repeated until a desired degree of accuracy is obtained, namely until the performance index satisfies the inequality

$$P \leqslant \epsilon, \quad (61)$$

where ϵ is a small number.

In our case $\epsilon = 10^{-10}$, i.e., we continued iterations until

$$P \leqslant 10^{-10}. \quad (62)$$

d. Application of the restoration algorithm for the enforcement of integral invariants of the shallow water equations

Here we will demonstrate the application of the restoration algorithm to our problem and in the process also emphasize the simplicity and adaptability of this algorithm.

1) We calculate the $(N \times 3)$ matrix $\mathbf{A}(\mathbf{x})$, which corresponds to $\phi_x(\mathbf{x})$.

Its entries are:

$$\begin{array}{lll} \dfrac{\partial\phi_1}{\partial u_{ij}} = 0 & \dfrac{\partial\phi_2}{\partial u_{ij}} = \dfrac{\Delta x}{2}(q_{i,j+1} - q_{i,j-1}) & \dfrac{\partial\phi_3}{\partial u_{ij}} = \Delta x \Delta y u_{ij} h_{ij} \\ \dfrac{\partial\phi_1}{\partial v_{ij}} = 0 & \dfrac{\partial\phi_2}{\partial v_{ij}} = \dfrac{\Delta y}{2}(-q_{i+1,j} + q_{i-1,j}) & \dfrac{\partial\phi_3}{\partial v_{ij}} = \Delta x \Delta y v_{ij} h_{ij} \\ \dfrac{\partial\phi_1}{\partial h_{ij}} = \Delta x \Delta y & \dfrac{\partial\phi_2}{\partial h_{ij}} = \dfrac{-\Delta x \Delta y}{2} q_{ij}^2 & \dfrac{\partial\phi_3}{\partial h_{ij}} = \dfrac{\Delta x \Delta y}{2}(u_{ij}^2 + v_{ij}^2 + 2gh_{ij}). \end{array} \quad (63)$$

We have omitted the subscript n for the time $n\Delta t$ for the sake of simplicity of notation. Also note that

$$q_{ij} = \frac{1}{h_{ij}} \left(\frac{v_{i+1,j} - v_{i-1,j}}{2\Delta x} - \frac{u_{i,j+1} - u_{i,j-1}}{2\Delta y} + f_j \right). \quad (64)$$

Having calculated $\mathbf{A}(\mathbf{x})$, we calculate the (3×3) matrix

$$\mathbf{B}(\mathbf{x}) = \mathbf{A}^{\mathrm{T}}(\mathbf{x})\mathbf{A}(\mathbf{x}) \tag{65}$$

$$\mathbf{B}(\mathbf{x}) = \begin{bmatrix} \sum_{ij}\left(\frac{\partial\phi_1}{\partial h_{ij}}\right)^2; & \sum_{ij}\frac{\partial\phi_1}{\partial h_{ij}}\frac{\partial\phi_2}{\partial h_{ij}}; & \sum_{ij}\frac{\partial\phi_1}{\partial h_{ij}}\frac{\partial\phi_3}{\partial h_{ij}} \\ \sum_{ij}\frac{\partial\phi_1}{\partial h_{ij}}\frac{\partial\phi_2}{\partial h_{ij}}; & \sum_{ij}\left[\left(\frac{\partial\phi_2}{\partial u_{ij}}\right)^2+\left(\frac{\partial\phi_2}{\partial v_{ij}}\right)^2+\left(\frac{\partial\phi_2}{\partial h_{ij}}\right)^2\right]; & \sum_{ij}\left(\frac{\partial\phi_2}{\partial u_{ij}}\frac{\partial\phi_3}{\partial u_{ij}}+\frac{\partial\phi_2}{\partial v_{ij}}\frac{\partial\phi_3}{\partial v_{ij}}+\frac{\partial\phi_2}{\partial h_{ij}}\frac{\partial\phi_3}{\partial h_{ij}}\right) \\ \sum_{ij}\frac{\partial\phi_1}{\partial h_{ij}}\frac{\partial\phi_3}{\partial h_{ij}}; & \sum_{ij}\left(\frac{\partial\phi_2}{\partial u_{ij}}\frac{\partial\phi_3}{\partial u_{ij}}+\frac{\partial\phi_2}{\partial v_{ij}}\frac{\partial\phi_3}{\partial v_{ij}}+\frac{\partial\phi_2}{\partial h_{ij}}\frac{\partial\phi_3}{\partial h_{ij}}\right); & \sum_{ij}\left[\left(\frac{\partial\phi_3}{\partial u_{ij}}\right)^2+\left(\frac{\partial\phi_3}{\partial v_{ij}}\right)^2+\left(\frac{\partial\phi_3}{\partial h_{ij}}\right)^2\right] \end{bmatrix}. \tag{66}$$

We then calculate the Lagrange multiplier vector (three components) λ, assuming $\alpha = 1$ and using formula (49), i.e.

$$\lambda = \mathbf{B}^{-1}(\mathbf{x})\phi(\mathbf{x}) \equiv [\mathbf{A}^{\mathrm{T}}(\mathbf{x})\mathbf{A}(\mathbf{x})]^{-1}\phi(\mathbf{x}). \tag{67}$$

3) We determine δx by calculating

$$\delta\mathbf{x} \equiv \mathbf{p} = -\mathbf{A}(\mathbf{x})\lambda \text{ (vector of length } N = 3N_xN_y) \tag{68}$$

and $\delta\mathbf{x} = \alpha\mathbf{p}$.

Then the restoration algorithm takes the same form as in section 3c.

e. *The spherical case*

In the spherical case our definitions of H^n, Z^n and E^n are, respectively

$$H = \frac{d\sin(d/2)}{\pi}\sum h_{ij}\cos\theta_j$$

$$Z = \frac{(ad)^2}{2}\sum\frac{\cos\theta_j}{h_{ij}}\left[\frac{v_{i+1,j}-v_{i-1,j}}{2ad\cos\theta_j}-\frac{u_{i,j+1}-u_{i,j-1}}{2ad}+f_j\right]^2,$$

$$E = \frac{(ad)^2}{2}\sum_{ij}(u_{ij}^2+v_{ij}^2+gh_{ij})h_{ij}\cos\theta_j, \tag{69}$$

where

$$d = \Delta\theta = \Delta\phi. \tag{70}$$

The term $d\sin(d/2)$ in H comes from a spherical area average and a is the radius of the earth. In such a case the entries of the $(N = 3)$ matrix $\mathbf{A}(\mathbf{x})$, which corresponds to $\phi_x(\mathbf{x})$, are:

$$\frac{\partial\phi_1}{\partial h_{ij}} = \frac{\partial H}{\partial h_{ij}} = \frac{d\sin(d/2)}{\pi}\cos\theta_j$$

$$\frac{\partial\phi_1}{\partial u_{ij}} = \frac{\partial\phi_1}{\partial v_{ij}} = 0$$

$$\frac{\partial\phi_2}{\partial u_{ij}} = \frac{ad}{2}\left[\frac{\cos\theta_{j+1}}{h_{i,j+1}}\left(\frac{v_{i+1,j+1}-v_{i-1,j+1}}{2ad\cos\theta_{j+1}}-\frac{u_{i,j+2}-u_{ij}}{2ad}+f_{j+1}\right)-\frac{\cos\theta_{j-1}}{h_{i,j-1}}\left(\frac{v_{i+1,j-1}-v_{i-1,j-1}}{2ad\cos\theta_{j-1}}-\frac{u_{ij}-u_{ij-2}}{2ad}+f_{j-1}\right)\right]$$

$$\frac{\partial\phi_2}{\partial v_{ij}} = \frac{ad}{2}\left[\frac{\cos\theta_{ij}}{h_{i-1,j}}\left(\frac{v_{ij}-v_{i-2,j}}{2ad\cos\theta}-\frac{u_{i-1,j+1}-u_{i-1,j-1}}{2ad}+f_j\right)-\frac{\cos\theta_j}{h_{i+1,j}}\left(\frac{v_{i+2,j}-v_{ij}}{2ad\cos\theta_j}-\frac{u_{i+1,j+1}-u_{i+1,j-1}}{2ad}+f_j\right)\right]$$

$$\frac{\partial\phi_2}{\partial h_{ij}} = -\frac{a^2d^2}{2}\frac{\cos\theta_j}{h_{ij}}\left[\frac{v_{i+1,j}-v_{i-1,j}}{2ad\cos\theta}-\frac{u_{i,j+1}-u_{i,j-1}}{2ad}+f_j\right]^2$$

$$\frac{\partial E}{\partial u_{ij}} = \frac{\partial\phi_3}{\partial u_{ij}} = a^2d^2u_{ij}h_{ij}\cos\theta_j$$

$$\frac{\partial E}{\partial v_{ij}} = \frac{\partial\phi_3}{\partial v_{ij}} = a^2d^2v_{ij}h_{ij}\cos\theta_j$$

$$\frac{\partial E}{\partial h_{ij}} = \frac{\partial\phi_3}{\partial h_{ij}} = \frac{a^2d^2}{2}(u_{ij}^2+v_{ij}^2+2gh_{ij})\cos\theta_j. \tag{71}$$

4. Numerical experiments

a. *Numerical results of long-term integrations*

Our hemispheric mesh consisted of a grid of (128×32) grid points, corresponding to a spacing of 2.8135° in $\Delta\theta$ and $\Delta\lambda$. The initial conditions were taken from a geostrophically balanced 500 mb level data with equivalent depth of 5 km.

A time step of 450 sec was used with the Turkel–Zwas scheme, with $p = 2$ and $q = 1$.

We first conducted hemispheric runs of the Turkel–Zwas scheme with realistic initial conditions for ten days, monitoring the conservation of total mass, total energy and potential enstrophy, respectively. As a decrease in the potential enstrophy was noted (see Fig. 1), we decided to carry out a second experiment in which the constraint restoration method was applied at each time step that a constraint violation, defined in terms of a predetermined relative change accuracy, was detected.

Figures 2 and 3 depict the behavior of the relative values of the total mass, potential enstrophy and total

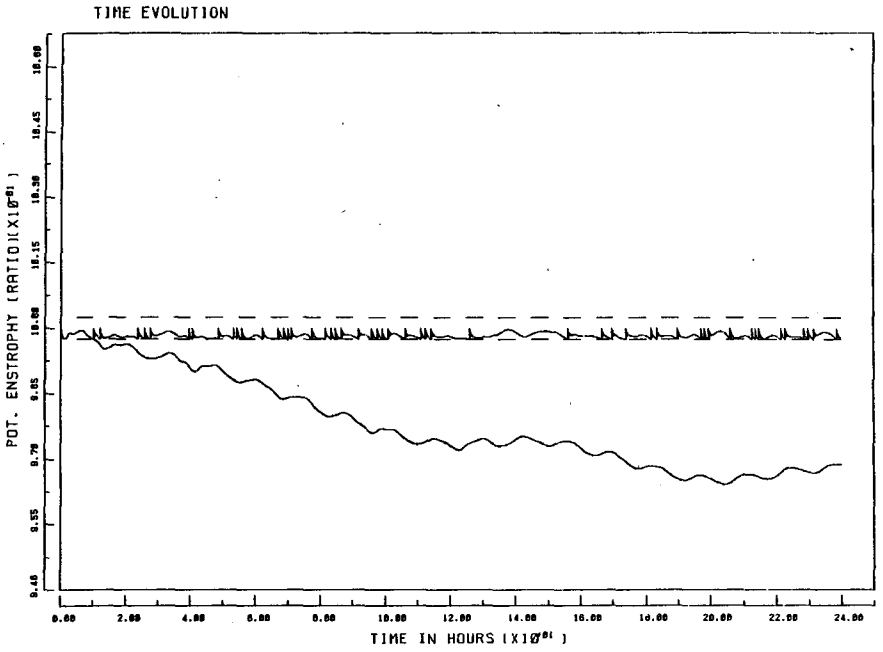

FIG. 1. Time variation of the potential enstrophy as function of its initial value without constraint restoration (continuous line) and with constraint restoration (quasi-constant spiky line). The dashed line delineates the limit acceptable for constraint violation.

energy normalized by their initial values for $p = 3$, $q = 1$ with and without application of the CRM method.

Figure 4 shows the initial height field, and Figs. 5, 6 and 7 show the height field after 2 days of integration with the Turkel–Zwas method with $p = 1$, $p = 2$ and $p = 3$, respectively, and $q = 1$ (with constraint resto-

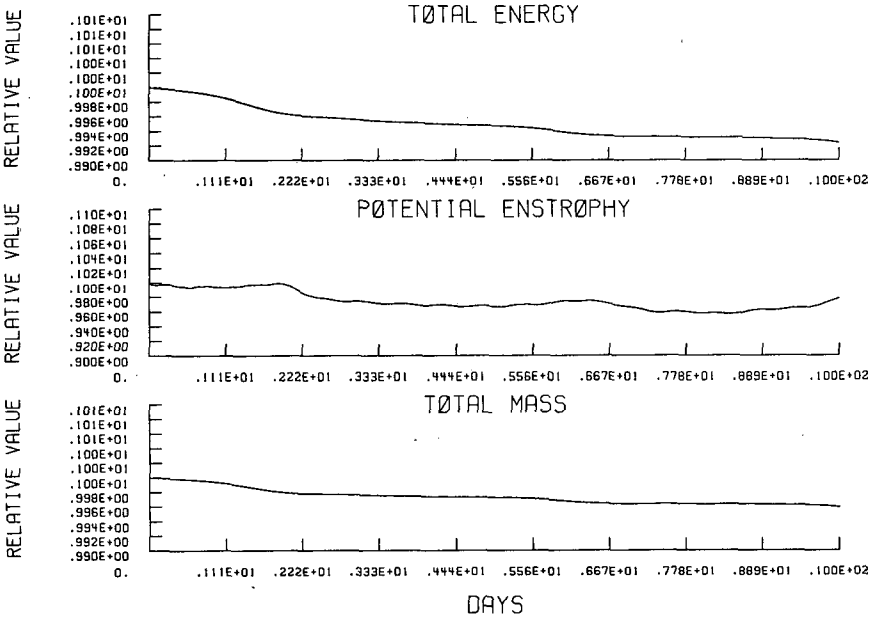

FIG. 2. The evolution of total energy, potential enstrophy and total mass, normalized by their initial values, as a function of time, for 10 days, for the T–Z hemispheric scheme with $p = 3$, $q = 1$. No constraint restoration applied.

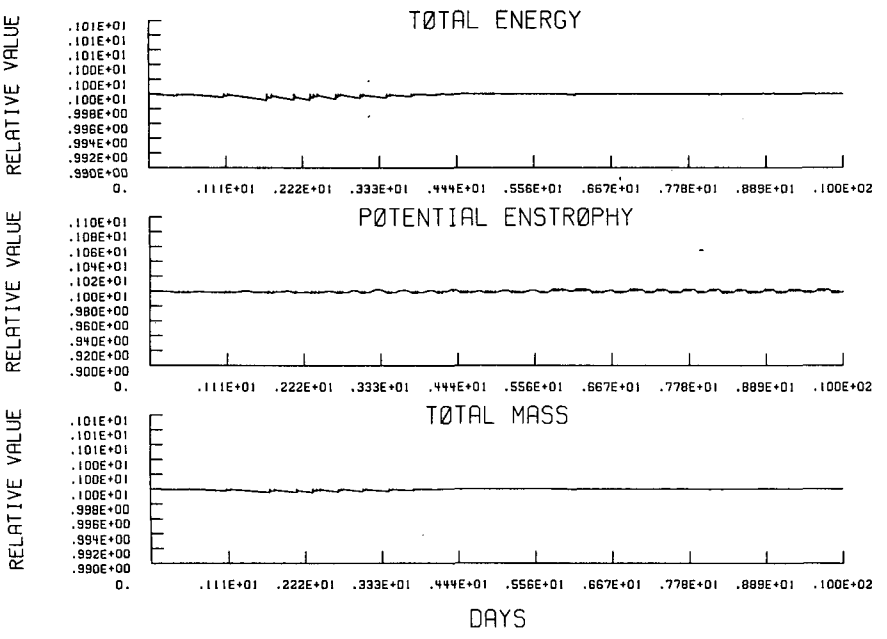

FIG. 3. The evolution of total energy, potential enstrophy and total mass, as in Fig. 2, for 10 days for the T–Z hemispheric scheme. The constraint restoration (CRM) applied.

ration applied at those time steps where a constraint violation was detected). Time-steps of 240 sec, 450 sec and 720 sec were used for $p = 1$ to $p = 3$, respectively.

Figures 8, 9 and 10 show the height field after 8 days of integration with the Turkel–Zwas method with $p = 1$, $p = 2$ and $p = 3$, respectively, and $q = 1$ and constraint restoration.

In another experiment we obtained the difference fields for a run of the Turkel–Zwas scheme with $p = 2$, $q = 1$ with and without application of the CRM method. The difference fields after 2 days and after 9 days are presented in Figs. 11 and 12.

Visual inspection shows that the impact of the constraint restoration becomes more important as the integration period augments. We have noticed that for long-term integrations and large time steps (9 days and longer), there was a tendency towards instability when the CRM method was not applied. More research is required in order to assess whether the CRM method improves long-term forecasts as there is no skill in barotropic models after two days.

b. *Computational efficiency of the constraint restoration algorithm*

In order to assess the computations efficiency of the constraint restoration algorithm, we performed a comparison between the Augmented Lagrangian algorithm (see Navon and de Villiers 1983) and the new algorithm for a typical repair time where we required that the three integral invariants of the shallow-water equations be satisfied and we measured the CPU time required for the full repair time.

For a partially vectorized version of the code run on the CDC-205, the CPU requested per time step of the model (for a time step of $\Delta t = 450$ sec) was 0.5 sec. During 10 days of integration we had a total of 157 repair times requesting, in total, 31.6 sec CPU when the CRM method was used, i.e., 0.2 sec for a repair time. The CRM was applied once every 14 time steps on the average. Application of an Augmented-Lagrangian nonlinear constrained optimization method (Navon and de Villiers (1983), Navon and de Villiers (1986) with the same accuracy criteria at the same repair points required 1.2 sec CPU time per repair, i.e., the use of the constraint restoration method results in a computational economy factor of 6.

The application of the Augmented-Lagrangian method of nonlinear constrained optimization produced almost identical results to the CRM and its results are therefore not displayed.

Thus, the use of the constraint restoration method results in a computational economy by a factor of 6. It should, however, be realized that we are only looking at a particular type of constrained minimization problem where, at a given time step, we are already in the vicinity of the minimum.

In other instances, when we are not in the vicinity of the minimum, the constraint restoration method loses its validity and we have to use the Augmented-Lagrangian method.

c. *Accuracy tests*

In order to provide a basis for comparison between the constraint restoration method applied to the Tur-

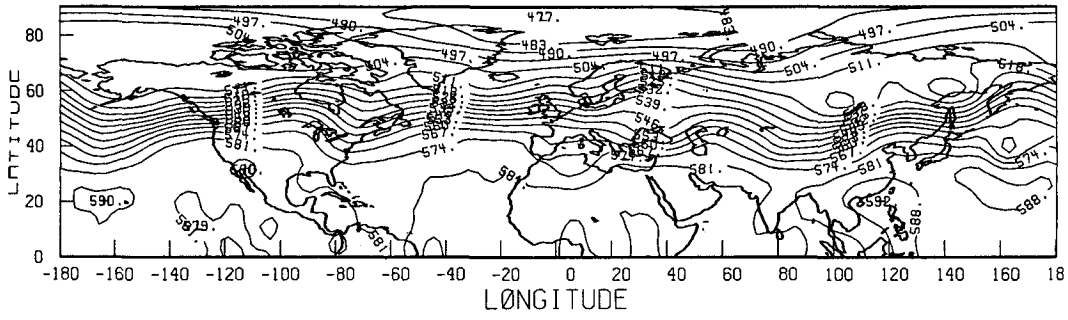

FIG. 4. Initial height field contours for the hemispheric T–Z scheme.

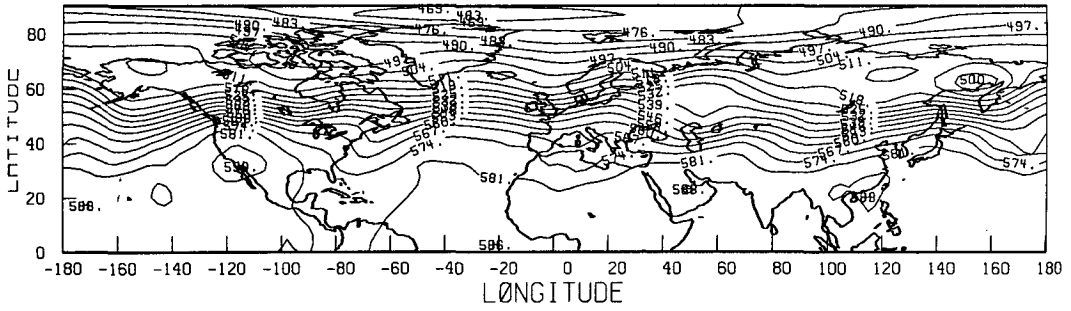

FIG. 5. Height field after 2 days of integration of the T–Z scheme for $p = 1$, $q = 1$ with constraint restoration method. ($\Delta t = 240$ sec).

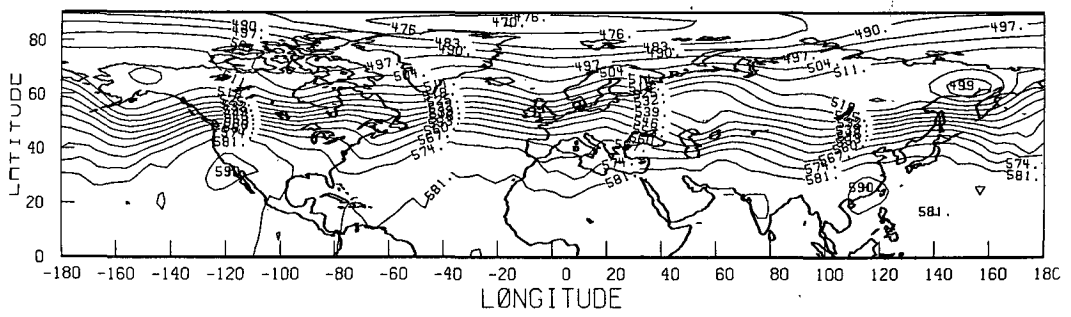

FIG. 6. As in Fig. 5, but for $p = 2$, $q = 1$ ($\Delta t = 450$ sec).

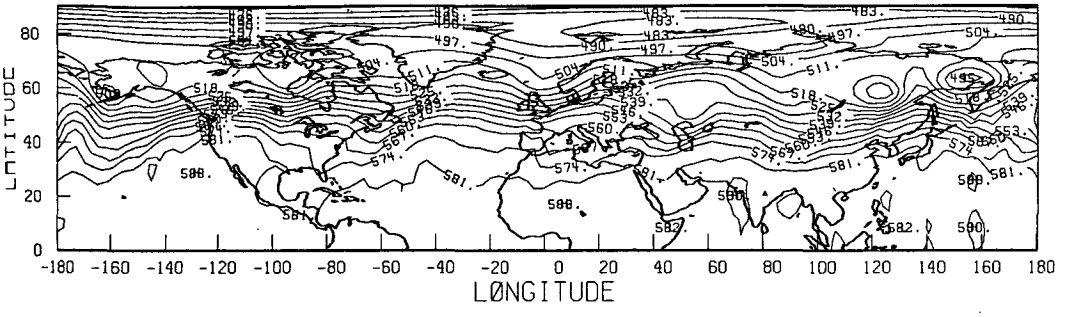

FIG. 7. As in Fig. 5 but for $p = 3$, $q = 1$ ($\Delta t = 720$ sec).

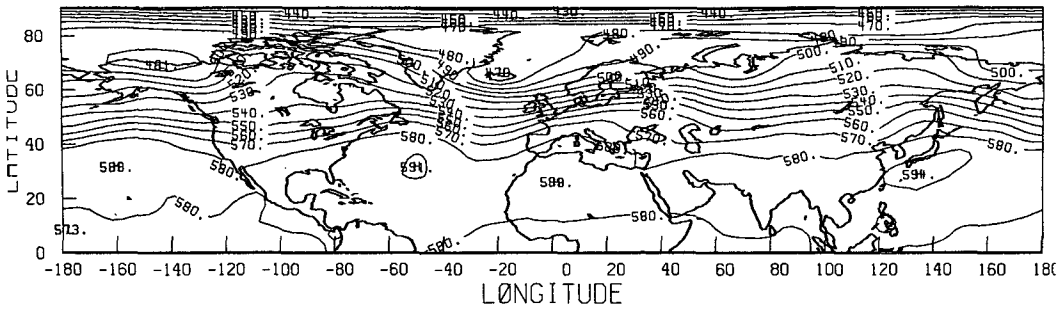

FIG. 8. Height field after 8 days with the T–Z scheme for $p = 1$, $q = 1$ ($\Delta t = 240$ sec).

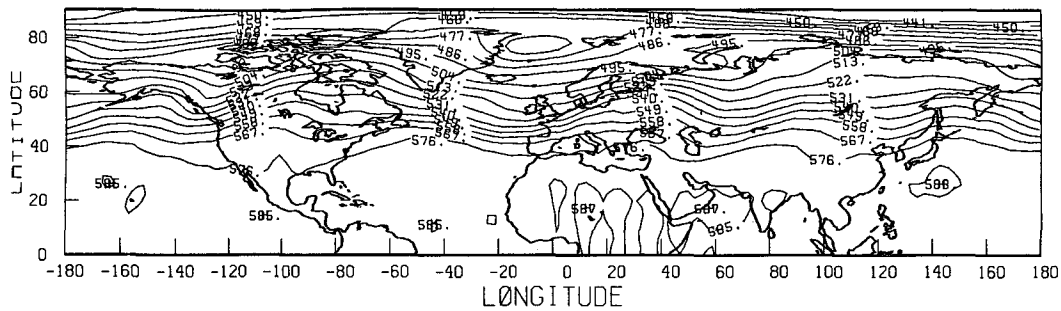

FIG. 9. As in Fig. 8 but for $p = 2$, $q = 1$ ($\Delta t = 450$ sec).

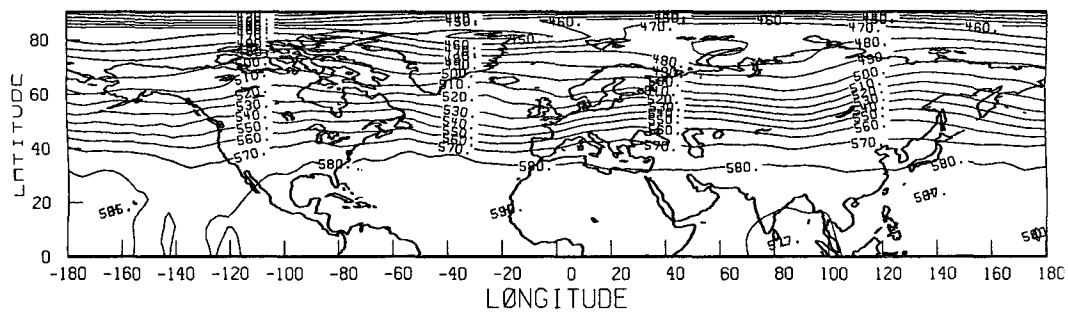

FIG. 10. As in Fig. 8 but for $p = 3$, $q = 1$ ($\Delta t = 720$ sec).

kel–Zwas hemispheric run and an unconstrained run of the same method—we used the same method as in Navon (1981), i.e. we assume the exact solution w_{EX} of the shallow-water equations to be a run of the Turkel–Zwas method computed with a fine discretization mesh refined by a factor of 2 for a latitude and longitude and a time step of 20 sec. The exact run did not use the constraint restoration method. The test shows that the relative error increases with p the coarseness factor, but that the application of the CRM method for enforcing conservation of the integral invariants slightly affects the relative error. Similar findings were found by Sasaki and Reddy (1980) when testing a variational method for enforcing conservation of potential enstrophy. They found a slight increase in the rms norm error.

The number of CRM corrections increased with the time step Δt, i.e., more corrections were needed for the case $p = 2$ than for the case $p = 1$. In all of the cases we used the Gustafsson (1971) relative error norm

$$\frac{\|E_{AP}\|}{\|W_{EX}\|} \tag{72}$$

and where $E_{AP} = W_{AP} - W_{EX}$, and

$$W = (u, v, \phi)_{ij}^{T}, \tag{73}$$

W_{AP} being the particular method compared to the "exact" run. The norm in (72) is defined by considering

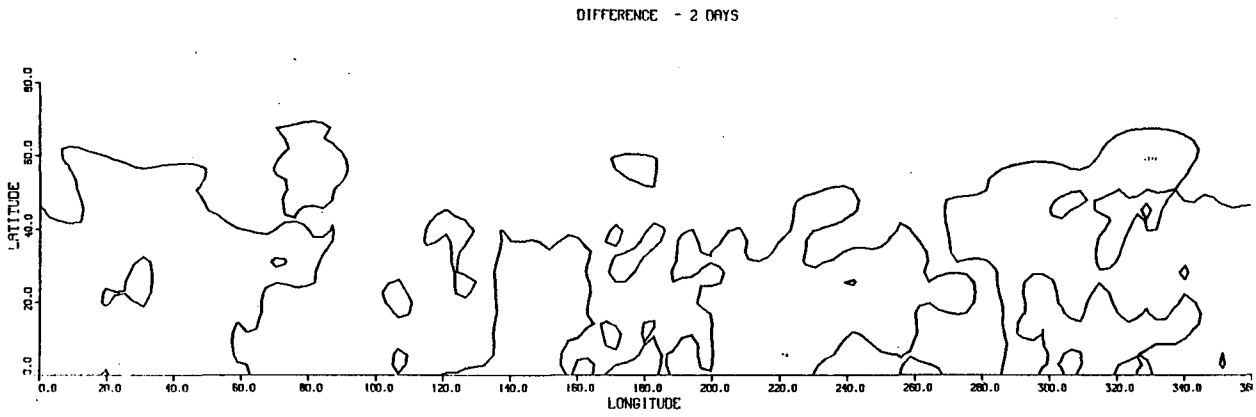

FIG. 11. Height difference field between hemispheric T–Z scheme with $p = 2$, $q = 1$ and constraint restoration method and without constraint restoration after 2 days. Contour interval is 50 m.

all vector functions of the form (73). The inner product of two vectors α and β is defined by

$$(\alpha, \beta) = \Delta x \Delta y \sum_{j=1}^{N_x} \{ \sum_{k=1}^{N_y - 1} \alpha_{jk}{}^T \beta_{jk} + \alpha_{j0}{}^T \beta_{jk} + \alpha_{j,N_y}^T \beta_j, N_y \} \tag{74}$$

and the norm by

$$\|\alpha\|^2 = (\alpha, \alpha). \tag{75}$$

Using $p = 2$ and $q = 1$ for the hemispheric run of the Turkel–Zwas method, we carried out a 48 h run with no constraint restoration—and one with a constraint restoration. In both cases we used the Gustafsson (1971) relative error norm (see Navon, 1981). We also tested the $p = 3$ and $q = 1$ case.

The results are given in the following:

TABLE 1. Relative error.

	$p = 1, q = 1$ $\Delta t = 240$ sec	$p = 2, q = 1$ $\Delta t = 450$ sec	$p = 3, q = 1$ $\Delta t = 720$ sec
No constraints after 48 h	0.1173×10^{-2}	0.3441×10^{-2}	0.4674×10^{-2}
With constraint restoration after 48 h	0.1335×10^{-2}	0.3752×10^{-2}	0.4518×10^{-2}

The constraint restoration method appears to affect the relative error only slightly (see Navon and de Villiers, 1983).

5. Conclusions

A space-splitting scheme, the Turkel–Zwas scheme, was applied to a hemispheric shallow-water equations model. When careful polar region treatment was applied, the method allowed the use of a time step almost 3 times larger than that allowed by the CFL condition for the explicit time integration leap-frog scheme. The T–Z method is the space alternative of the time-splitting or split-explicit time integration methods which use different time steps for the slow Rossby-wave generating terms and the fast gravity-wave generating terms. Application of a constraint restoration method due to Miele et al. (1969) and which is equivalent to the Bayliss–Isaacson (1975) conservative method has proved to be very efficient and computationally economical for our case.

Issues for further research should concern first the applicability of the Turkel–Zwas space-splitting scheme in operational models and its computational efficiency versus the split-explicit method of Gadd (1978a, 1978b). As was pointed out by E. Turkel (personal communication) the T–Z scheme will perform better if starting from normal-mode initialized conditions, with periodic application (every 12 h or so) of the normal mode initialization. Another issue to be addressed is the total phase error for the different scales of motion due to the use of different grids for the gravity-wave generating terms and the Rossby waves, respectively, of the T–Z scheme. The use of the CRM method prevented nonlinear instability in long-term runs. As was pointed out by Gadd (1978) conservation of mass, total energy and enstrophy is significant for medium-range forecasts (4–10 days) and their preservation constituted a problem in long-term integrations for the split-explicit integration scheme, unless the Coriolis term was treated implicitly. The use of different resolution grids for problems with different time scales, provides a new perspective for meteorological problems when explicit time-differencing schemes are used, and it is hoped that this paper should stimulate research in this field.

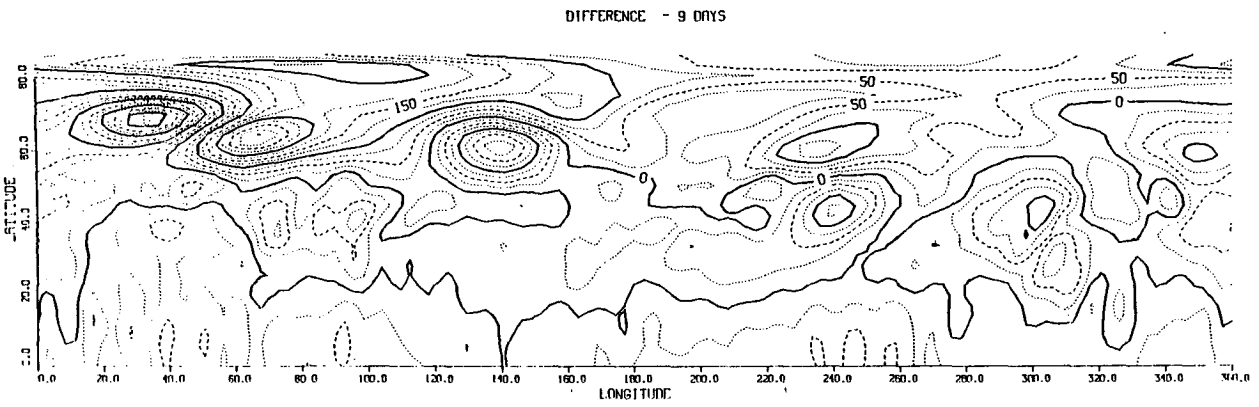

FIG. 12. As in Fig. 11 but after 9 days and with a contour interval of 50 m.

Acknowledgments. The first author acknowledges Professor A. Miele of Rice University, Houston, Texas, for some instructive discussions concerning the CRM method. Thanks are also due to Professor E. Isaacson from the Courant Institute, for his contribution to the proof of equivalence between the CRM method and the Bayliss–Isaacson method. We should also like to thank Professor E. Turkel of Tel-Aviv University for private communications as well as for his generosity in making available a code for this method.

Mr. James Meritt of the Mesoscale Air–Sea Interaction Group helped with the graphics, and Ms. Mimi Burbank's expert typing rendered our manuscript into a legible paper.

APPENDIX A

Proof of Stability Condition for the Turkel–Zwas Method

Let us consider a stability analysis of the shallow-water equations and let us for simplicity assume $f = 0$. If we approximate the shallow-water equations by a centered difference approximation of leap-frog type, we obtain (see Kreiss and Oliger, 1973)

$$w(t+\Delta t) = w(t-\Delta t) - 2\Delta t \begin{pmatrix} u & 0 & 1 \\ 0 & u & 0 \\ \phi & 0 & u \end{pmatrix} D_{0x} w(t) - 2\Delta t \begin{pmatrix} v & 1 & 0 \\ \phi & v & 0 \\ 0 & 0 & v \end{pmatrix} D_{0y} w(t) \quad \text{(A1)}$$

where

$$w(t) = (u(x,y,t), v(x,y,t), \phi(x,y,t)) \quad \text{(A2)}$$

denotes the solution of the difference equations and D_{0x} and D_{0y} are the central difference approximations in the x and y directions, respectively, i.e.

$$D_{0x} u_{ij}^n = \frac{u_{i+1,j}^n - u_{i-1,j}^n}{2\Delta x}, \quad D_{0y} u_{ij}^n = \frac{u_{i,j+1}^n - u_{i,j-1}^n}{2\Delta y}. \quad \text{(A3)}$$

If we consider the equations (A1) with constant coefficients by replacing the coefficient matrices in (A1) by

$$\begin{pmatrix} u_0 & 0 & 1 \\ 0 & u_0 & 0 \\ \phi_0 & 0 & u_0 \end{pmatrix} \text{ and } \begin{pmatrix} v_0 & 1 & 0 \\ \phi_0 & v_0 & 0 \\ 0 & 0 & v_0 \end{pmatrix} \quad \text{(A4)}$$

where $u_0, v_0, \phi_0 > 0$ represent a constant flow.

To symmetrize the problem let us introduce a new variable

$$\mu = \begin{pmatrix} 1 & 0 & 0 \\ 0 & 1 & 0 \\ 0 & 0 & \sqrt{\phi_0} \end{pmatrix} w. \quad \text{(A5)}$$

And our difference approximation (A1) becomes

$$\mu(t+\Delta t) = \mu(t-\Delta t) - w\Delta t Q_0 \mu(t) \quad \text{(A6)}$$

where

$$Q_0 = \begin{pmatrix} u_0 & 0 & \phi_0^{1/2} \\ 0 & u_0 & 0 \\ \phi_0^{1/2} & 0 & u_0 \end{pmatrix} D_{0x} + \begin{pmatrix} v_0 & \phi_0^{1/2} & 0 \\ \phi_0^{1/2} & v_0 & 0 \\ 0 & 0 & v_0 \end{pmatrix} D_{0y} \quad \text{(A7)}$$

and it has now symmetric coefficients.

Using a theorem of Kreiss and Oliger (1973, p. 36) we know that the approximation is stable if

$$\Delta t \|Q_0\| < 1 \quad \text{(A8)}$$

where the norm of Q_0 is given by

$$\|Q_0\| = (Q, Q)^{1/2} \tag{A9}$$

and (,) is the L_2 scalar product.

Let us take the Fourier transform of $\Delta t\|Q_0\|$, $\Delta t\|\hat{Q}_0\|$ (we know that $\Delta t\|Q_0\| = \Delta t\|\hat{Q}_0\|$ by Parseval's relation).

The eigenvalues of $\Delta t\hat{Q}_0$ are

$$\kappa_1 = \frac{i\Delta t}{h}(u_0 \sin\xi + v_0 \sin\eta) \tag{A10}$$

$$\kappa_{2,3} = \frac{i\Delta t}{h}\{u_0 \sin\xi + v_0 \sin\eta \pm [\sqrt{\phi_0(\sin^2\xi + \sin^2\eta)}]\} \tag{A11}$$

where

$$h = \Delta x = \Delta y, \quad \xi = w\Delta x = wh, \quad \eta = w\Delta y = wh \tag{A12}$$

and w is the real dual variable to x. Then

$$\kappa\|\hat{Q}_0\| = \max_j|\kappa_j| \leqslant \frac{\Delta t}{h}(|u_0| + |v_0| + \sqrt{2\phi_0}) \tag{A13}$$

and the approximation is stable if

$$\frac{\Delta t}{h} < \frac{1}{|u_0| + |v_0| + \sqrt{2\phi_0}} \tag{A14}$$

If we use the Turkel–Zwas method, i.e., we differentiate the ϕ terms over a grid p times coarser we obtain for the ϕ terms:

$$D_{0px}\phi = \phi_0 \frac{e^{ipw} - e^{-ipw}}{2\Delta xp} = \frac{i \sin\xi p}{p} \tag{A15}$$

$$D_{0py}\phi = \phi_0 \frac{e^{ipw} - e^{-ipw}}{2\Delta yp} = \frac{i \sin\eta p}{p} \tag{A16}$$

$$\Delta t\|\hat{Q}_0\| = \max_j|\kappa_j| \leqslant \frac{\Delta t}{h}\left(|u_0| + |v_0| + \frac{\sqrt{2\phi_0}}{p}\right), \tag{A17}$$

and the approximation is stable if

$$\frac{\Delta t}{h} < \frac{1}{|u_0| + |v_0| + (\sqrt{2\phi_0}/p)}. \tag{A18}$$

This concludes the proof for Eq. (9).

APPENDIX B

Relation between CRM and the Bayliss–Isaacson Method

When we minimize Eq. (33) subject to the constraints $\phi(\mathbf{x}^*) = 0$, then the problem is equivalent to

$$\min_{\forall\delta\mathbf{x},\lambda}\left[\frac{1}{2}\delta\mathbf{x}^{\mathrm{T}}\delta\mathbf{x} + \lambda^{\mathrm{T}}\phi(\mathbf{x} + \delta\mathbf{x})\right]. \tag{B1}$$

Taking the minimum with respect to λ gives

$$\frac{\partial}{\partial\lambda_l}(\mathrm{B1}) = \phi_l(\mathbf{x} + \delta\mathbf{x}) = 0 \quad 1 \leqslant l \leqslant p \tag{B2}$$

and taking the minimum with respect to δx_k we obtain

$$\frac{\partial}{\partial\delta x_k}|\mathrm{B1}| = \delta x_k + \sum_{r=1}^{p}\lambda_r\frac{\partial\phi_r}{\partial\delta x_k}(\mathbf{x} + \delta\mathbf{x}) = 0, \quad 1 \leqslant k \leqslant N. \tag{B3}$$

(B3) is approximated by expanding about $\delta\mathbf{x} = \mathbf{0}$:

$$\begin{pmatrix}\delta x_1\\ \delta x_2\\ \vdots\\ \delta x_N\end{pmatrix} + \sum_{r=1}^{p}\begin{pmatrix}\frac{\partial\phi_r}{\partial x_1}(\mathbf{x})\\ \frac{\partial\phi_r}{\partial x_2}(\mathbf{x})\\ \vdots\\ \frac{\partial\phi_r}{\partial x_N}(\mathbf{x})\end{pmatrix} = 0. \tag{B4}$$

This is the same as the corrective function of Bayliss–Isaacson (see Navon, 1981)

$$\mathbf{V}(n+1) = \sum_{k=1}^{p}\alpha_k \operatorname{grad} G_k + \mathbf{P} \tag{B5}$$

with $P = 0$, if $\alpha_r = -\lambda_r$ for $1 \leqslant r \leqslant p$. This proof has been suggested by Prof. E. Isaacson.

REFERENCES

Arakawa, A., and V. R. Lamb, 1977: Computational design of the basic dynamical processes of the U.C.L.A. general circulation model. *Methods in Computational Physics.*, Vol. 17, Academic Press, 174–265.

Bayliss, A., and E. Isaacson, 1975: How to make your algorithm conservative. *Notices of the Amer. Math. Soc.*, **22**, No. 5, A594–A595.

Burridge, D. M., 1975: A split semi-implicit reformulation of the Bushby-Thompson 10 level model. *Quart. J. Roy. Meteor. Soc.*, **101**, 777–792.

Daley, R., 1980: The development of efficient time integration schemes using model normal modes. *Mon. Wea. Rev.*, **108**, 100–110.

Gadd, A., 1978a: A split-explicit integration scheme for numerical weather prediction. *Quart. J. Roy. Meteor. Soc.*, **104**, 569–582.

——, 1978b: A numerical advection scheme with small phase speed errors. *Quart. J. Roy. Meteor. Soc.*, **104**, 583–594.

Gustafsson, B., 1971: An alternating direction implicit method for solving the shallow-water equations. *J. Comput. Phys.*, **7**, 239–252.

Haltiner, G. J., and R. T. Williams, 1980: *Numerical Prediction and Dynamic Meteorology*, Wiley & Sons, 477 pp.

Isaacson, E., 1977: Integration schemes for long-term calculation. In *2nd IMACS (IACA) Meeting on Advances in Computer Methods for Partial Differential Equations*, R. Vichnevetsky, Ed., AICA, 251–255. [International symposium on computer methods for partial differential equations, Lehigh University, Bethlehem, PA 18015, 392 pp.]

Kalnay, E., R. C. Balgovind, W. Chao, J. Edelman, J. Pfaendtner, L. Takacs and K. Takano, 1983: Documentation of the GLAS fourth-order general circulation model. NASA Tech. Memor. 86064, Greenbelt, MD, 20771.

Kreiss, H. O., and J. Oliger, 1973: Methods for the approximate solution of time dependent problems. *GARP Publ. Ser. No. 10*, 107 pp. [Available from World Meteorological Organization, C.P. 5, C4-1221, Geneva 20, Switzerland.]

Magazenkov, L. M., M. Ye. Shvets and B. Ye Shneyerov, 1971: The distributed analysis approach to integration of equations of dynamics of a barotropic fluid over a long time interval. Isvestya, Academy of Sciences, U.S.S.R., *Atmos. Oceanic Phys.*, **7**, English Edition, 560–564. [Published by the American Geophysical Union and American Meteorological Society, 2000 Florida Ave., N.W., Washington, D.C., 20009.]

Miele, A., and J. C. Heideman, 1968: The restoration of constraints in holonomic problems. Aero Astronautics Rep. No. 39, Rice University, 14 pp.

——, —— and J. N. Damoulakis, 1969a: The restoration of constraints in holonomic and non-holonomic problems. *J. Optimiz. Theory Appl.*, **3**(5), 361–381.

——, H. Y. Huang and J. C. Heideman, 1969b: Sequential gradient restoration algorithm for the minimization of constrained functions. Ordinary and conjugate-gradient versions. *J. Optimiz. Theory Appl.*, **4**(4), 213–243.

——, A. V. Levy and E. E. Cragg, 1971: Modifications and extensions of the conjugate-gradient-restoration algorithm for mathematical programming problems. *J. Optimiz. Theory and Appl.*, **7, No. 6,** 450–472.

Navon, I. M., 1981: Implementation of '*a posteriori*' methods for enforcing conservation of potential enstrophy and mass in discretized shallow-water equations models. *Mon. Wea. Rev.*, **109, No. 5,** 946–958.

——, and R. de Villiers, 1983: Combined penalty multiplier optimization methods to enforce integral invariants conservation. *Mon. Wea. Rev.*, **111**(6), 1228–1243.

——, and ——, 1986: GUSTAF: A quasi-Newton nonlinear ADI Fortran IV program for solving the shallow-water equations with Augmented-Lagrangians. *Comput. Geosci.* **12(2),** 151–173.

Robert, A., 1979: The semi-implicit method in numerical methods used in atmospheric models. *GARP Publ. Ser. Part II,* **17,** Chapter 4, 499 pp. [Available from World Meteorological Organization, C.P. 5, C4-1221, Geneva 20, Switzerland.]

Sasaki, Y., 1976: Variational design of finite-difference schemes for initial value problems with an integral invariant. *J. Comput. Phys.*, **21,** 270–278.

——, 1977: Variational design of finite-difference schemes for initial value problems with a global divergent barotropic model. *Contrib. Atmos. Phys.*, **50,** 284–289.

——, and J. N. Reddy, 1980: A comparison of stability and accuracy of some numerical models of two-dimensional circulation: *Int. J. Numer. Meth. Eng.*, **16,** 149–170.

Takacs, L. L., 1986: Documentation of the Goddard Laboratory for Atmospheres four-order two-layer shallow-water model. NASA Tech. Memo. 86227, 80 pp. [NASA/GSFC, Greenbelt, MD 20771.]

——, and R. Balgovind, 1983: High-latitude filtering in global grid point models. *Mon. Wea. Rev.*, **111**(10), 2005–2015.

——, E. Kalnay and I. M. Navon, 1985: High-latitude filtering in a global gridpoint model using model normal modes. *Proc. Seventh Conf. on Numerical Weather Prediction,* Montreal, Amer. Meteor. Soc., 277–283.

Turkel, E., and G. Zwas, 1979: Explicit large-time-step schemes for the shallow-water equations. *Proc. Third Int. Symp. in Advances in Computer Methods for Partial Differential Equations,* R. Vichnevetsky and R. S. Stepleman, Eds., Publications IMACS, Lehigh University, 65–69, 442 pp.